



# Lead-free BaBi<sub>4</sub>Ti<sub>4</sub>O<sub>15</sub> ceramics: Effect of synthesis methods on phase formation and electrical properties

J.D. Bobić<sup>a,\*</sup>, M.M. Vijatović Petrović<sup>a</sup>, N.I. Ilić<sup>a</sup>, E. Palaimiene<sup>b</sup>, R. Grigalaitis<sup>b</sup>, C.O. Paiva-Santos<sup>c</sup>, M. Cilence<sup>c</sup>, B.D. Stojanović<sup>a</sup>

<sup>a</sup>Institute for Multidisciplinary Research, Belgrade University, Belgrade, Serbia

<sup>b</sup>Faculty of Physics, Vilnius University, Vilnius, Lithuania

<sup>c</sup>Instituto de Química-UNESP, Araraquara, S.P., Brazil

Received 3 July 2014; received in revised form 12 August 2014; accepted 19 August 2014

Available online 28 August 2014

## Abstract

The processing of ferroelectric BaBi<sub>4</sub>Ti<sub>4</sub>O<sub>15</sub> (BBT) ceramics from powders prepared by conventional solid state reaction (SSR) and mechanochemical activation (MA) has been investigated. It was shown that MA synthesis reduces the synthesis temperature of BBT powders, leading to smaller particles with reduced anisotropy and consequently to smaller grain size of ceramics. Dielectric properties were investigated in a wide range of temperatures (20–800 °C) and frequencies (1.21 kHz to 1 MHz). The relative dielectric permittivity at Curie temperature was higher for solid state obtained ceramics than for the mechanically treated ones. The conductivity of sintered samples was studied, suggesting decreasing of conductivity of BBT-MA in comparison with BBT-SS ceramics. The influence of the grain and the grain boundaries contribution to the dielectric behavior in both ceramics was analyzed through impedance spectroscopy. A well-defined ferroelectric hysteresis loop was obtained for both samples.

© 2014 Elsevier Ltd and Techna Group S.r.l. All rights reserved.

**Keywords:** A. Powders: solid state reaction; B. Grain boundaries; C. Electrical conductivity; C. Ferroelectric properties

## 1. Introduction

The BaBi<sub>4</sub>Ti<sub>4</sub>O<sub>15</sub> (BBT) is a member of the family of ferroelectric oxides with an Aurivillius-type structure [1]. The crystal structure of this material consists of four perovskite layers separated by bismuth oxide sheets. In comparison with almost isotropic (cubic) structure of BT, PMN and PZT [2–4], intrinsic electrical properties of Aurivillius type of compounds are anisotropic with the maximum value of conductivity and the major component of spontaneous polarization parallel to the (Bi<sub>2</sub>O<sub>2</sub>)<sup>2+</sup> layers [5]. The main problem in application of bismuth titanate based ceramics for many devices is its high conductivity. Oxygen vacancies, which are main conductive species in bismuth layered compounds, can be suppressed by donor doping [6–9] or grain size

reduction [5,10–12]. As miniaturization of electronic devices demands smaller particle size of powders with controlled morphology, the desired characteristics of the starting powder has become a critical issue.

BBT has been prepared through various methods like conventional solid state method [11–15], sol–gel [16], co-precipitation [17–19], the polymeric precursors-Pechini process [20]. Mechanochemical synthesis of fine-grained Aurivillius structure powders has shown that it is possible to form Aurivillius structure at low temperatures [21–23]. Mechanical activation is a process during which, from the viewpoint of changes of free energy, changes in the amount of accumulated energy occur. This technique skips multiple steps of calcinations at elevated temperatures, which leads to smaller particles with reduced anisotropy or even equiaxial, and provides an improved chemical homogeneity. Many Aurivillius-type materials have been prepared by the mechanical activation in different type of

\*Corresponding author. Tel.: +381 11 2085 039; fax: +381 11 2085 062.

E-mail address: [jelenabobic@yahoo.com](mailto:jelenabobic@yahoo.com) (J.D. Bobić).

the mills. Single phase of nanocrystalline  $\text{Bi}_4\text{Ti}_3\text{O}_{12}$  was formed after 15 h of milling in a planetary ball mill by Kong and co-authors [24] while Stojanovic et al. obtained  $\text{Bi}_4\text{Ti}_3\text{O}_{12}$  after 6 h [25].  $\text{CaBi}_4\text{Ti}_4\text{O}_{15}$  and  $\text{SrBi}_4\text{Ti}_4\text{O}_{15}$  with nanometer size were directly synthesized from their oxide mixtures after milling in high energy shaker mill for 30 h and 20 h, respectively [21,22].

It is known that the dielectric and polar properties and the nature of phase transitions in ceramics are very sensitive to their microstructure. Considering that the grain size affects conductivity of Aurivillius compounds, this paper deals with the effect of mechanochemical assisted synthesis method on electrical, dielectric, ferroelectric and conductive properties of  $\text{BaBi}_4\text{Ti}_4\text{O}_{15}$  compounds. The lack of reports in mechanically activated BBT has prompted the authors to synthesize  $\text{BaBi}_4\text{Ti}_4\text{O}_{15}$  compound by mechanochemical synthesis and compare the phase formation of BBT compounds in both mechanochemical and solid state reaction methods.

## 2. Experimental procedure

### 2.1. Preparation of ceramics

$\text{BaBi}_4\text{Ti}_4\text{O}_{15}$  was prepared by the conventional solid-state reaction method. Stoichiometric amounts of high purity oxides:  $\text{BaO}$ ,  $\text{TiO}_2$  and  $\text{Bi}_2\text{O}_3$  (Alfa Aesar, p.a. 99%) were homogenized in isopropanol medium for 24 h in a planetary ball mill (Fritsch Pulverisette 5). The obtained powder was calcined at  $950^\circ\text{C}$  for 4 h. As prepared powder is denoted as BBT-SS.

In parallel to the solid state preparation of powders, stoichiometric amounts of appropriate high purity oxides were milled for 2, 4, 6 h in air atmosphere in a planetary ball mill (Fritsch Pulverisette 5). The rotational speed of the disk was 325 rpm and the speed of the vials was about 400 rpm. Tungsten carbide grinding balls (approx. 10 mm in diameter) and two cylindrical bowls (75 mm in diameter, 65 mm in height) were used. Based on those values the ball-impact energy was  $\Delta E_b^* = 51.5$  mJ/hit. The weight-normalized cumulative energy which was introduced to the system during milling until the BBT phase was formed ( $E_{\text{cum}} = 566.1$  kJ/g) were calculated according to the assumption proposed and elaborated by Burgio et al. [26]. Ball-to-powder weight ratio was 30:1. The 6 h-milled powder was calcined at  $850^\circ\text{C}$  for 4 h to obtain well crystallized BBT structure. The powder and ceramic samples obtained by mechanochemical synthesis are denoted as BBT-MA samples. Both, BBT-SS and BBT-MA powders were pressed into pellets at 98 MPa and 294 MPa respectively using a uniaxial press. The reason for different pressure for powder compacting is because BBT-SS powder is not possible to compacting at the pressure higher than 98 MPa, due to it is getting leafed which is caused by specific powder morphology (discussed in Item 3). The finer and better homogenized MA powder could be compacted at higher pressure because of the spherical particles that have better packing degree, so the compacting at 294 MPa is possible in that case.

Ceramic samples were prepared by conventional sintering at  $1120^\circ\text{C}$  for 1 h (Lenton-UK oven). The sintering was performed in sealed alumina crucibles in order to avoid bismuth loss. Heating rate was  $3^\circ\text{C}/\text{min}$ , with the natural cooling in air atmosphere. The relative densities of the BBT-SS and BBT-

MA pellets were determined to be  $\sim 89$  and  $93\%$ , respectively. Slightly larger density of BBT-MA sample may be a consequence of the higher compacting pressure and better homogenization of BBT-MA powder.

### 2.2. Characterization methods

The formation of phase and crystal structure of obtained BBT ceramics was verified using a conventional X-ray diffract meter (XRD, Model D5000, Siemens) with  $\text{CuK}\alpha$  radiation,  $2\theta$  range between  $20^\circ$  and  $70^\circ$ , step size of  $0.02^\circ$  ( $2\theta$ ), divergence slit = 0.5 mm, receiving slit = 0.3 mm. The density of obtained ceramics was calculated from the geometrical measurements of samples and weight. The morphology and microstructure of obtained powders and ceramics were examined using scanning

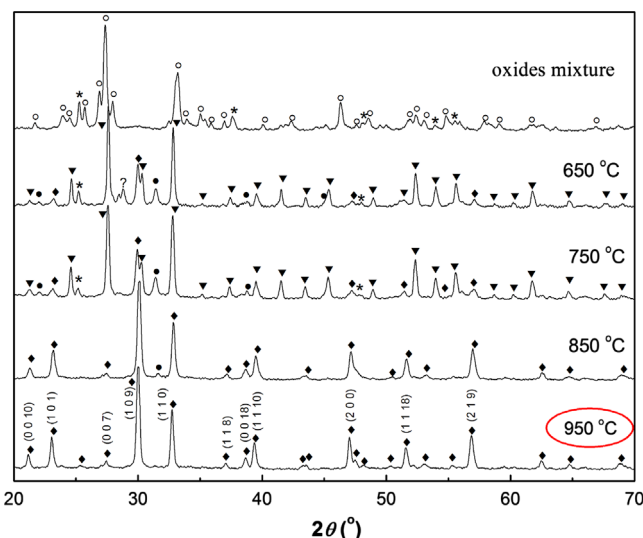


Fig. 1. Diffraction patterns of the 24 h homogenized starting mixture of oxides and powders obtained by calcination of the starting mixture at different temperatures for 4 h (○),  $\text{Bi}_2\text{O}_3$  (\*),  $\text{TiO}_2$  (●),  $\text{BaTiO}_3$  (?), unidentified phase (▼),  $\text{Bi}_{12}\text{Ti}_2\text{O}_{20}$  (◆), Aurivillius phase.

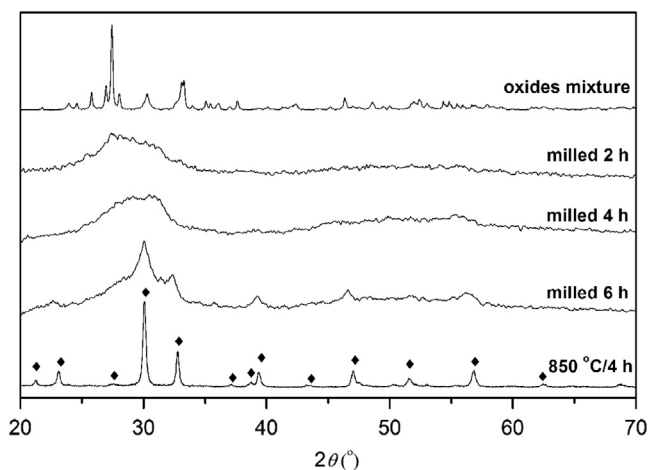


Fig. 2. XRD traces of homogenized starting oxide mixture together with mechanically activated powders (for 2, 4 and 6 h) and calcinated powder at  $850^\circ\text{C}$  for 4 h.

electron microscope (FE-SEM, Jeol JSM 6330F and SEM, TESCAN SM-300). Samples were prepared for electrical measurements by coating the polished surfaces of the ceramics with the platinum paste and firing at 750 °C to form the electrodes. The electrical measurements (dielectric constant, dielectric losses and impedance analysis) were performed using a HP 4284A in the 1.21 kHz–1 MHz frequency range and temperature interval from 20 °C to 727 °C. The temperature was controlled with a programmable oven with an accuracy of 1 °C. Impedance results were analyzed using commercially available Z-View software.

### 3. Results and discussion

Homogenized equivalent mixture of starting oxides was calcined at different temperatures in the range 650–950 °C for

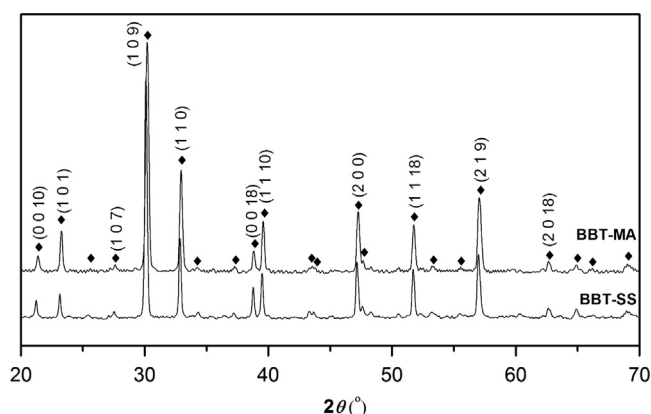


Fig. 3. XRD patterns of BBT ceramics processed from (a) solid state reaction method, BBT-SS and (b) mechanochemical activated method BBT-M.

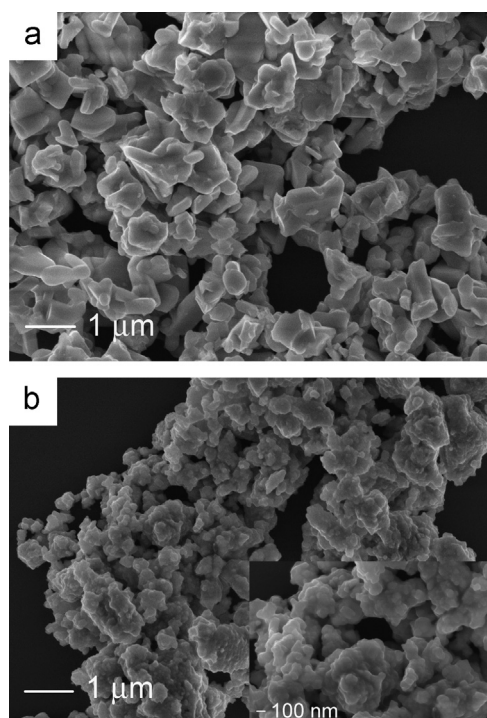


Fig. 4. Field emission scanning electron micrographs: (a) BBT-SS and (b) BBT-MA powder.

4 h in order to monitor the dynamics of the formation of the  $\text{BaBi}_4\text{Ti}_4\text{O}_{15}$  powders. Complete XRD analysis is shown in Fig. 1. Sharp peaks of crystalline  $\text{Bi}_2\text{O}_3$  and  $\text{TiO}_2$  could be observed in the 24 h-homogenized oxide mixture. Calcination of the starting mixture at temperature of 650 °C led to the formation of a new phase, which was identified as silenite phase  $\text{Bi}_{12}\text{TiO}_{20}$ . In addition to silenite phase, barium titanate and Aurivillius phase were also formed. At the calcination temperature of 750 °C there was no significant difference compared to the lower calcination temperature. Powder diffraction pattern confirmed that the formation of the layered Aurivillius phase was completed at 850 °C with the presence of a small amount of  $\text{BaTiO}_3$  (BT) as a secondary phase. Finally, a pure BBT phase was found in the specimen after calcination at 950 °C for 1 h. Hence, it can be concluded that the main mechanism of BBT formation is:



Formation of pure, crystalline BBT phase was confirmed by comparing diffraction lines with JCPDS card No. 35-0757. Chakrabarti et al. [19] have reported the same formation mechanism of BBT prepared by chemical method after calcination of precursor powders at 1000 °C for 4 h.

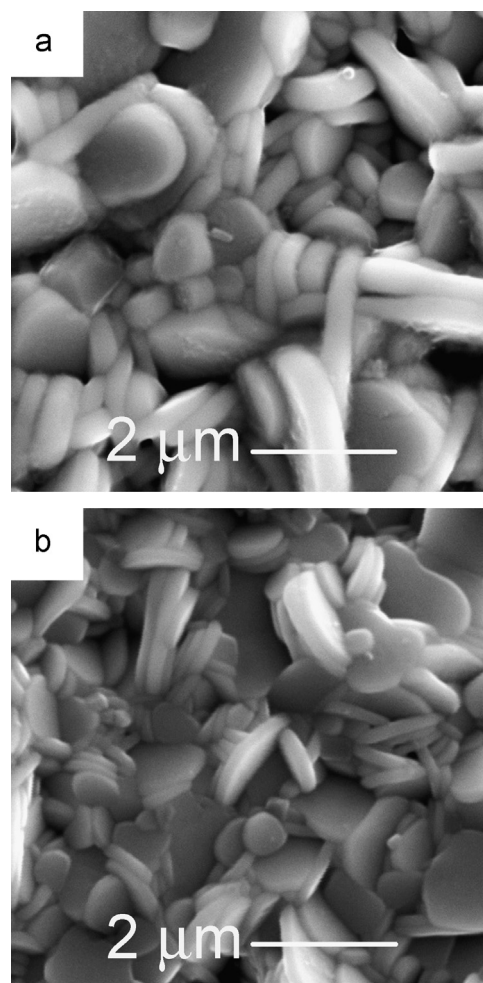


Fig. 5. SEM images of (a) BBT-SS, (b) BBT-MA ceramics on the free surface.

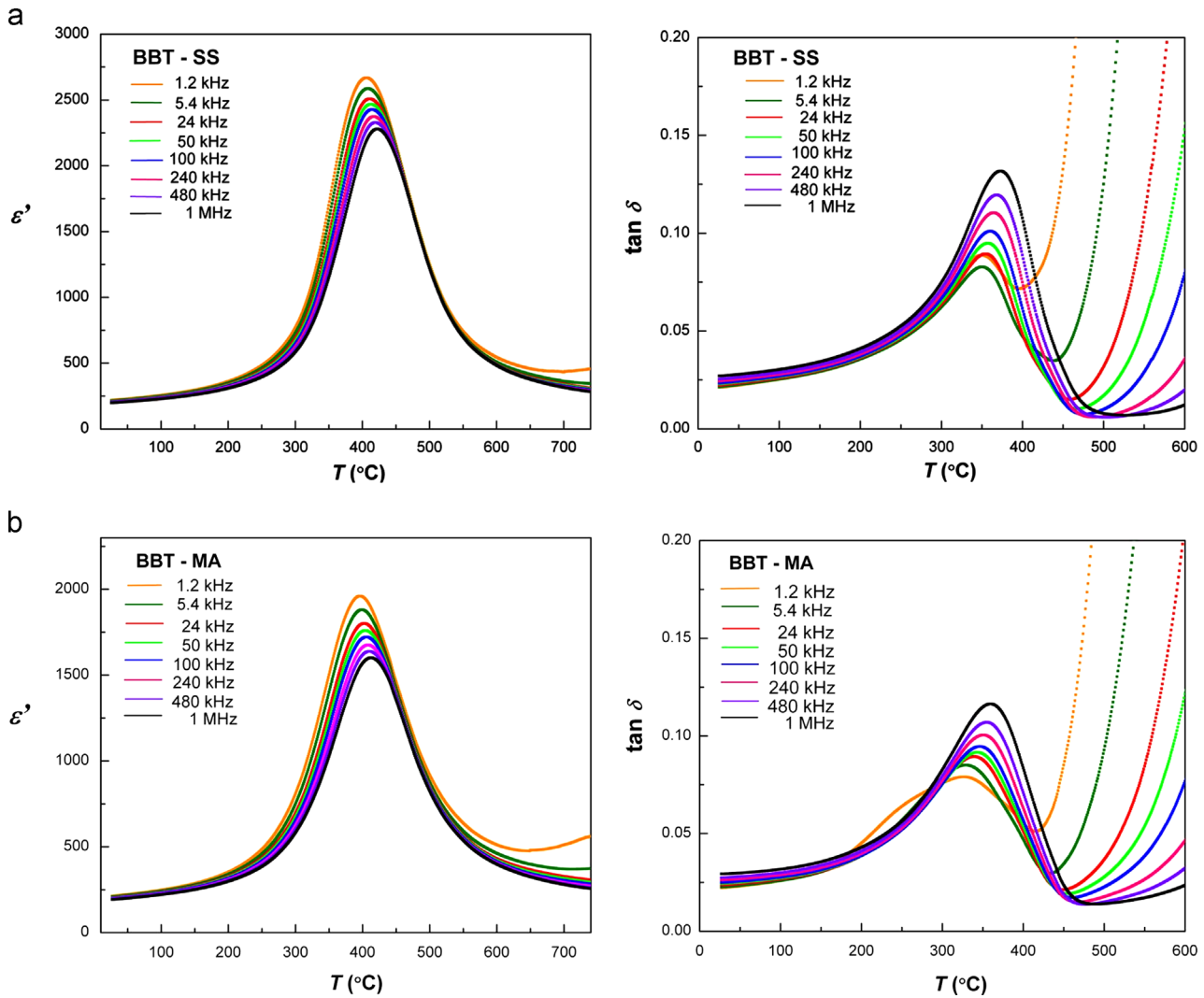


Fig. 6. Dielectric permittivity as a function of temperature for BBT-SS and BBT-MA ceramics.

Table 1  
Some relaxor parameters of BBT-SS and BBT-MA ceramics.

Samples	$\epsilon_{RT}$	$\tan \delta_{RT}$	$\epsilon_m$	$T_m$ (°C)	$\Delta T_{relax}$
BBT-SS	205	0.024	2429	415	16.3
BBT-MA	200	0.025	1723	404	16.9

Fig. 2 shows the XRD traces of homogenized starting oxide mixture of BaO, Bi<sub>2</sub>O<sub>3</sub> and TiO<sub>2</sub> together with those mechanically activated for 2, 4 and 6 h, respectively. Sharp peaks of crystalline Bi<sub>2</sub>O<sub>3</sub> and TiO<sub>2</sub> were observed in the starting oxides mixture. No BaO is detected, as the added amount is rather small. The disappearances of sharp peaks of oxides and subsequent formation of broadened peak, which confirms the formation of highly amorphous powders, have taken place after just 2 h of milling. The similar XRD data were observed after 4 h of milling. For the composition mechanically activated for 6 h characteristic diffraction peaks of Aurivillius phase were established. The powder was further calcined at 850 °C for 4 h to obtain well crystallized BBT powder (Fig. 2). Although mechanochemical activation allows the

synthesis of BBT powders at just 100 °C lower temperature than by SSRs method, significantly smaller particles with reduced anisotropy are obtained by MA method as it will be shown below.

Sintering of the both powders at 1120 °C for 1 h after pressing resulted in the generation of single phase barium bismuth titanate ceramics as confirmed by X-ray analysis (Fig. 3).

Particle size, shape and degree of agglomeration are important characteristics of powder and have great impact on the development of microstructure (i.e. grain size of synthesized materials), and, therefore, other physical and electrical properties of polycrystalline ceramics [27,28]. BBT-SS and BBT-MA powders were analyzed by scanning electron microscopy and the significant differences were found in the form and size of particles (Fig. 4). The FE-SEM observation of the BBT-SS powders (Fig. 4a) showed the presence of particles with mostly lamellar shape as a consequence of high temperature of calcination at 950 °C. The average particle size was around 450 nm. Fig. 4b. shows that BBT-MA powder was consisted of smaller particles, mostly rounded, in the range of 100–150 nm. It is obvious that both powders are agglomerated. The conventional method requires a high calcination temperature, leading to

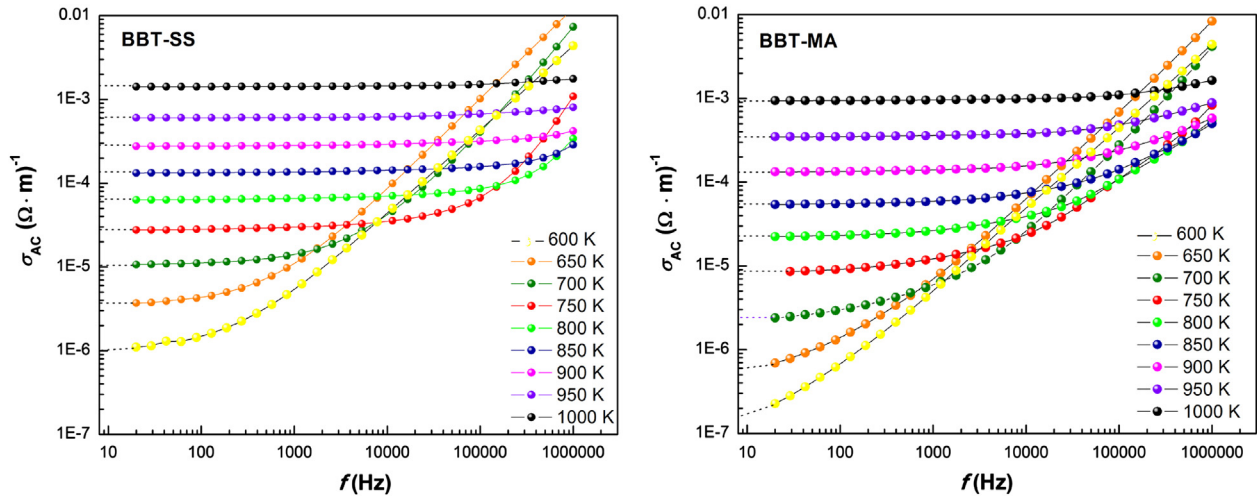


Fig. 7. Variation of ac conductivity with frequency at different temperatures for BBT-SS and BBT-MA compounds.

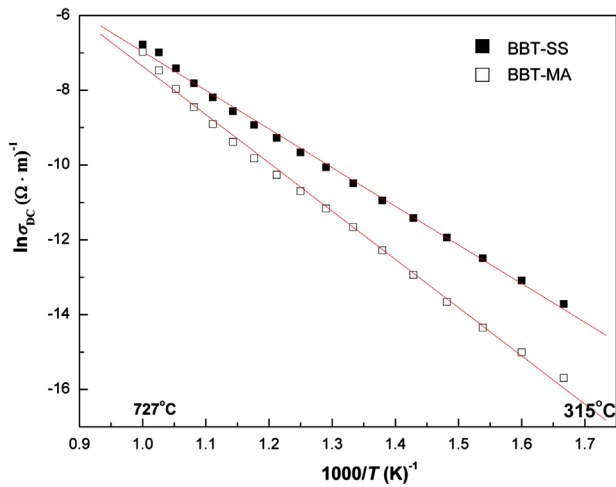


Fig. 8. Arrhenius plots of dc conductivity of BBT-SS and BBT-MA ceramics.

Table 2  
Conductivity at different temperatures for BBT-SS and BBT-MA ceramics.

Temp (°C)	BBT-SS, $\sigma_g$ ( $\Omega \text{ m}$ ) <sup>-1</sup>	BBT-MA $\sigma_g$ ( $\Omega \text{ m}$ ) <sup>-1</sup>
377	$3.44 \times 10^{-6}$	$5.35 \times 10^{-7}$
477	$2.74 \times 10^{-5}$	$8.49 \times 10^{-6}$
577	$1.33 \times 10^{-4}$	$5.46 \times 10^{-5}$
677	$6.01 \times 10^{-4}$	$3.48 \times 10^{-4}$
727	$1.43 \times 10^{-3}$	$9.36 \times 10^{-4}$

inevitable hard particle coarsening while agglomeration of mechanochemically treated powders is consequence of the reduction in particle sizes.

Crystalline structure of Aurivillius compounds generally promotes a platelike morphology, with platelets growing preferentially in the basal plane (*ab* plane). As a result, properties of the polycrystalline materials are strongly affected by their microstructure, especially by the orientation of the platelike grains and by the length to thickness ratio (aspect ratio) of the grains [5,7].

Micrographs of the free surfaces of the BBT-SS and BBT-MA ceramics are shown in Fig. 5. Both samples were consisted of randomly arranged laminar grains, which are typical for this type of structure. The average grain size of BBT-SS ceramics could be determined from SEM micrographs, and it was around 2–3  $\mu\text{m}$  in length and 0.5  $\mu\text{m}$  in thickness. In comparison with the BBT-SS, reduction in the average grain size of BBT-MA ceramic is due to the decrease in the particle size of the milled powders. Average grain of BBT-MA ceramics was around 1.0  $\mu\text{m}$  in length and 0.2  $\mu\text{m}$  in thickness.

The temperature dependence of the dielectric constant of the BBT-SS and BBT-MA specimens at different frequencies are shown in Fig. 6. From previously published papers [23,29] it is known that pure BBT ceramics acts like a ferroelectric relaxor with broad transition around 400 °C. Similar to the materials with perovskite structure, the relaxor behavior in the Bi-layered compounds is attributed to a structural disorder, which is either inherent or induced by doping. Relaxor behavior of  $\text{BaBi}_4\text{Ti}_4\text{O}_{15}$  originates from anti-site defects, where the  $\text{Bi}^{3+}$  ions enter A-site, while  $\text{Ba}^{2+}$  are incorporated into  $(\text{Bi}_2\text{O}_2)^{2+}$  layers [30]. The degree of relaxation behavior, obtained by formula  $\Delta T_{\text{relax}} = T_m$  (1.21 MHz) –  $T_m$  (1 kHz) was found to be 16.3 K for the BBT-SS and 16.9 K for the BBT-MA samples. BBT showed  $\Delta T_{\text{relax}}$  comparable to values observed for PMN (~20 K), PLZT (8/65/35) (~25 K) [31] and related Ba-based layered perovskite relaxors [32]. According to results of  $\Delta T_{\text{relax}}$ , synthesis method did not influence on relaxation process which confirms that the degree of structural distortion is the same in both ceramics. The Curie temperature ( $T_C$ ) was found to decrease in BBT-MA in comparison to BBT-SS samples. This was possibly due to the decrease in crystallite size of mechanochemically treated sample.

By means of most of the authors [33,34] the dielectric constant should increase with decreasing the grain size in most perovskite materials, and then decrease with further decrease of the grain size. Contrast to that, Ferrer and coauthors have found that Aurivillius  $\text{SrBi}_4\text{Ti}_4\text{O}_{15}$  ceramics with the highest platelet size shows the largest dielectric permittivity [35]. Recent investigation

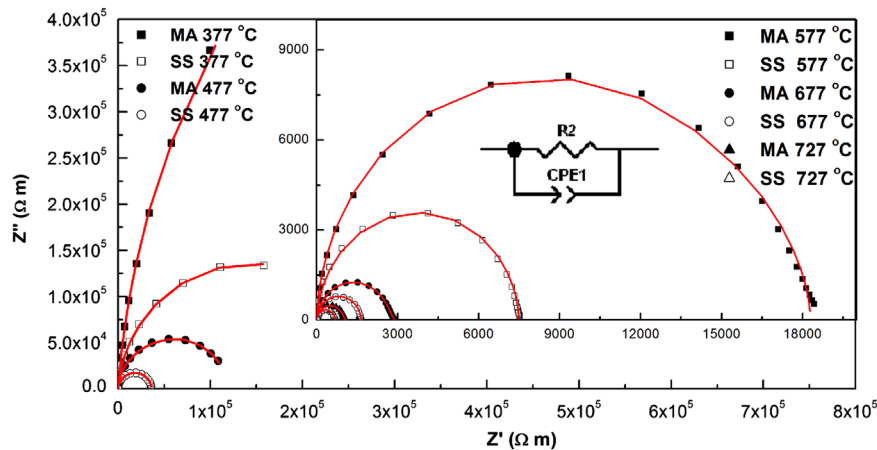
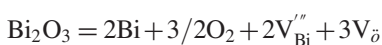


Fig. 9. Complex impedance plot of the BBT-SS and BBT-MA ceramics at different temperatures.

of the grain size-dependent electrical properties of  $\text{Bi}_4\text{Ti}_3\text{O}_{12}$  ceramics showed that when the grain size is changing from  $4.2 \mu\text{m}$  to  $1.65 \mu\text{m}$ , dielectric constant at  $T_C$  slightly decreases. When the grain size is further reduced to  $0.57 \mu\text{m}$ , increase of the dielectric constant at  $T_C$  is observed. In our investigation, the dielectric permittivities for both samples of BBT at room temperature were very close to each other (Table 1). The higher value of the permittivity close to the ferroelectric phase transition of the BBT-SS samples in comparison with BBT-MA could be explained by brick-wall model, where the high permittivity grains are isolated by low permittivity grain boundaries [36]. With higher contribution of grain boundaries in BBT-MA, the permittivity was lower.

The *ac* conductivity ( $\sigma_{AC}$ ) of the BBT ceramic materials at different temperatures was calculated using the relation  $\sigma_{AC} = \epsilon_o \epsilon_r \tan \delta$ , where the symbols have their usual meanings. The frequency dependence of  $\sigma_{AC}$  of the materials in high temperature range of  $327 \text{ }^\circ\text{C}$  to  $727 \text{ }^\circ\text{C}$  is shown in Fig. 7. DC conductivity data can be theoretically predicted from extrapolation of *ac*-conductivity data on *y*-axis from  $\sigma_{AC}$  vs. frequency plot. The obtained values of  $\sigma_{DC}$  at different temperatures enable determination of the activation energy for conduction process ( $E_{DC}$ ) according to the Arrhenius law:  $\sigma_{DC} = \sigma_o \exp(-E_{DC}/kT)$ . This is graphically presented in Fig. 8 as  $\ln(\sigma_{DC})$  vs.  $1000/T$ . The values of activation energies, calculated by linear fitting of the data points were  $0.89 \text{ eV}$  and  $1.11 \text{ eV}$  for BBT-SS and BBT-MA ceramics, respectively. At high temperature the conductivity in Aurivillius-type ceramics is dominated by intrinsic defects—migration of oxygen vacancies which generation is related with the evaporation of Bi:



The activation energies for conductivity for both samples were close to  $1 \text{ eV}$ , which is attributed to the oxygen vacancies related phenomena [11].

As has been mentioned, the bismuth-based layered compounds possess a relatively high electrical conductivity in the *ab* plane, which makes difficult the poling of the ceramics, and therefore the existence of piezoelectric response. It is well

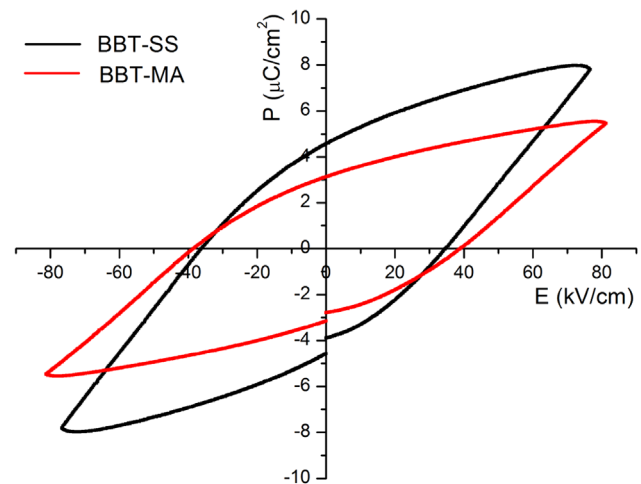


Fig. 10. Ferroelectric hysteresis loop recorded at room temperature for BBT-SS and BBT-MA ceramics.

known that the conductivity in the direction of *ab* plane is higher than that parallel to the *c*-axis [5]. Therefore, the smaller the aspect ratio (i.e. contribution of the *ab* planes), the lower the conductivity of the BBT ceramics is. This was confirmed in our investigation, where the mechanochemical synthesis method reduced the electrical conductivity in comparison with the solid state prepared ceramics by the reduction of grain size. The decreased conductivity could also be attributed to the increase in the number of grain boundaries with grain size decreasing, resulting onto an increase in scattering of charge carriers at grain boundaries. Values of conductivity for both samples at different temperatures are presented in Table 2.

Fig. 9 shows the impedance data at several temperatures as a Nyquist diagram. At low temperature the plots tended to form a straight line with the large slope indicating insulating behavior of the samples. As the temperature was increased, the slope of the curves was decreased, bowing towards the real axis. Red semicircular arcs are fitting curves calculated by ZView software. Although more pronounced influence of grain boundaries on impedance measurement of BBT-MA samples was expected

(appearance of at least one more semicircle or depressed semicircular arc), only a single semicircle was observed in both BBT ceramic. This showed that the grains have main contribution to the conduction in both ceramics. Lower conductivity of BBT-MA grains could be related to the smaller contribution of *ab* planes in the conductivity with decreasing the grain size or possible “filling” of some oxygen vacancies influencing the lowering of carrier concentration in this ceramics.

The *P*–*E* hysteresis loops at 100 Hz frequency and maximum electric field of 80 kV/cm were measured at room temperature for the both BBT ceramics and they are shown in Fig. 10. The ferroelectric behavior is clearly observable. The remnant polarization (*P<sub>r</sub>*) and coercive field (*E<sub>c</sub>*) were 4.54 μC/cm<sup>2</sup>, 34.4 kV/cm and 3.08 μC/cm<sup>2</sup>, 39.0035 kV/cm for BBT-SS and BBT-MA respectively. *P<sub>r</sub>* was decreased with decreased grain size because the reduced number of domain variants in the smaller grains lowers domain wall mobility. *E<sub>c</sub>* was increased with decreased grain size, which was ascribed to the higher internal stresses in fine grain ceramics [37].

#### 4. Conclusions

BBT ceramics were successfully prepared by the solid state and mechanochemical synthesis in order to analyze effect of processing on its electrical properties. A single Aurivillius phase was confirmed by X-ray diffraction after sintering for both samples. Mechanochemical synthesis route allowed the powder synthesis to be performed at lower temperatures than in the case of the SSR, which led to smaller particles of MA powders. As a consequence, SEM micrographs confirmed that the grain size of mechanochemically obtained ceramics was smaller than that obtained by the solid state reaction method. According to results of  $\Delta T_{\text{relax}}$ , synthesis method did not influence the relaxation process, which confirmed that the same degree of structural disorder exists in both ceramics. Similar to other Aurivillius compounds, it was confirmed that conductivity decreases with reduction of the grain size, which was attributed to the increase in the number of grain boundaries. Lowering of remnant polarization with decreasing grain size was observed.

#### Acknowledgements

The results presented in this paper are realized with the financial support of Ministry of Education, Science and Technological Development of the Republic of Serbia (which is also providing scholarship for the co-author Nikola Ilić) through the project III 45021 and COST MP 0904. Special thanks to M.Sc. Nikola Tasic from Institute for Multidisciplinary Research, Belgrade University for ferroelectric measurements.

#### References

- [1] B. Aurivillius, Mixed bismuth oxides with layer lattices, III. Structure of BaBi<sub>4</sub>T<sub>4</sub>O<sub>15</sub>, Ark. Kemi 1 (1950) 519–527.
- [2] M.M. Vijatovic, J.D. Bobic, B.D. Stojanovic, Hystory and challenges of barium titanate: Part II, Sci. Sinter. 40 (2008) 235–244.
- [3] J. Portelles, N.S. Almodovar, J. Fuentes, O. Raymond, J. Heiras, J.M. Siqueiros, ac Conductivity in Gd doped Pb(Zr<sub>0.53</sub>Ti<sub>0.47</sub>)O<sub>3</sub> ceramics, J. Appl. Phys. 104 (2008) 073511.
- [4] R. Ranjan, R. Kumar, B. Behera, R.N.P. Choudhary, Effect of Sm on structural, dielectric and conductivity properties of PZT ceramics, Mater. Chem. Phys. 115 (2009) 473–477.
- [5] T. Jardiell, A.C. Caballero, M. Villegas, Aurivillius ceramics, Bi<sub>4</sub>Ti<sub>3</sub>O<sub>12</sub>-based piezoelectrics, J. Ceram. Soc. Jpn. 116 (2008) 511–518.
- [6] L. Zhang, R. Chu, S. Zhao, G. Li, Q. Yin, Microstructure and electrical properties of niobium doped Bi<sub>4</sub>Ti<sub>3</sub>O<sub>12</sub> layer-structured piezoelectric ceramics, Mater. Sci. Eng., B 116 (2005) 99–103.
- [7] H.S. Shulman, D. Damjanović, N. Setter, Niobium doping and dielectric anomalies in bismuth titanate, J. Am. Ceram. Soc. 83 (3) (2000) 528–532.
- [8] J.D. Bobić, M.M. Vijatović Petrović, J. Banys, B.D. Stojanović, Electrical properties of niobium doped barium bismuth–titanate ceramics, Mater. Res. Bull. 47 (2012) 1874–1880.
- [9] I. Pribošič, D. Makovec, M. Drofenik, Electrical properties of donor- and acceptor-doped BaBi<sub>4</sub>Ti<sub>4</sub>O<sub>15</sub>, J. Eur. Ceram. Soc. 21 (2001) 1327–1331.
- [10] M. Alguero, P. Ferrer, E. Vila, J.E. Iglesias, A. Castro, Bi<sub>4</sub>Ti<sub>3</sub>O<sub>12</sub> ceramics from powders prepared by alternative routes: wet no-coprecipitation chemistry and mechanochemical activation, J. Am. Ceram. Soc. 89 (11) (2006) 3340–3347.
- [11] A. Moure, A. Castro, L. Pardo, Aurivillius-type ceramics, a class of high temperature piezoelectric materials: Drowbacks, advantage and trends, Prog. Solid State Chem. 37 (2009) 15–39.
- [12] M. Villegas, A.C. Caballero, C. Moure, P. Duran, J.F. Fernandez, Factor affecting the electrical conductivity of donor-doped Bi<sub>4</sub>Ti<sub>3</sub>O<sub>12</sub> piezoelectric ceramics, J. Am. Ceram. Soc. 89 (9) (1999) 2411–2416.
- [13] P. Fang, H. Fan, J. Li, L. Chen, F. Liang, The microstructure and dielectric relaxor behavior of BaBi<sub>4-x</sub>La<sub>x</sub>Ti<sub>4</sub>O<sub>15</sub> ferroelectric ceramics, J. Alloys Compd 497 (2010) 416–419.
- [14] S. Kumar, K.B.R. Varma, Dielectric relaxation in bismuth layer-structured BaBi<sub>4</sub>Ti<sub>4</sub>O<sub>15</sub> ferroelectric ceramics, Curr. Appl. Phys. 11 (2011) 203–210.
- [15] J.D. Bobic, M.M. Vijatović Petrović, J. Banys, B.D. Stojanović, Effect of La substitution on the structural and electrical properties of BaBi<sub>4-x</sub>La<sub>x</sub>Ti<sub>4</sub>O<sub>15</sub>, Ceram. Int. 39 (2013) 8049–8057.
- [16] D. Xie, W. Pan, Study on BaBi<sub>4</sub>Ti<sub>4</sub>O<sub>15</sub> nanoscaled powders prepared by sol–gel method, Mater. Lett. 57 (2003) 2970–2974.
- [17] A. Chakrabati, J. Bera, T.P. Sinha, Dielectric properties of BaBi<sub>4</sub>Ti<sub>4</sub>O<sub>15</sub> ceramics produced by cost-effective chemical method, Physica B 404 (2009) 1498–1502.
- [18] S.K. Rout, E. Sinha, A. Hussian, J.S. Lee, S.W. Ahn, I.W. Kim, S.I. Woo, Phase transition in ABi<sub>4</sub>Ti<sub>4</sub>O<sub>15</sub> (A=Ca, Sr, Ba) Aurivillius oxides prepared through a soft chemical route, J. Appl. Phys. 105 (2009) 024105.
- [19] A. Chakrabarti, J. Bera, T.P. Sinha, Dielectric properties of BaBi<sub>4</sub>Ti<sub>4</sub>O<sub>15</sub> ceramics produced by cost-effective chemical method, Physica B 404 (2009) 1498–1502.
- [20] A.V. Murugan, S.C. Navale, V. Ravi, Preparation of nanocrystalline ferroelectric BaBi<sub>4</sub>Ti<sub>4</sub>O<sub>15</sub> by Pechini method, Mater. Lett. 60 (2006) 1023–1025.
- [21] M.H. Sim, J.M. Xue, J. Wang, Layer structured calcium bismuth titanate by mechanical activation, Mater. Lett. 58 (2004) 2032–2036.
- [22] S.H. Ng, J.M. Xue, J. Wang, High temperature piezoelectric strontium bismuth titanate from mechanical activation of mixed oxides, Mater. Chem. Phys. 75 (2002) 131–135.
- [23] J.D. Bobic, M.M. Vijatovic, S. Greicius, J. Banys, B.D. Stojanovic, Dielectric and relaxor behavior of BaBi<sub>4</sub>Ti<sub>4</sub>O<sub>15</sub> ceramics, J. Alloys Compd. 499 (2010) 221–226.
- [24] L.B. Kong, J. Ma, W. Zhu, O.K. Tan, Preparation of Bi<sub>4</sub>Ti<sub>3</sub>O<sub>12</sub> ceramics via a high-energy ball milling process, Mater. Lett. 51 (2001) 108–114.
- [25] B.D. Stojanovic, C.O. Paiva-Santos, C. Jovalekic, A.Z. Simoes, F.M. Filho, Z. Lazarevic, J.A. Varela, Mechanically activating formation of layered structured bismuth titanate, Mater. Chem. Phys. 96 (2006) 471–476.
- [26] N. Burgio, A. Iasonna, M. Magini, S. Martelli, F. Padella, Il Nuovo Cimento 13D (4) (1991) 459.

- [27] M.M. VijatovicPetrovic, J.D. Bobic, H. Ursic, J. Banys, B.D. Stojanovic, The electrical properties of chemically obtained barium titanate improved by attrition milling, *J. Sol Gel Sci.* 67 (2013) 267–272.
- [28] H. Chen, B. Shen, J. Xu, J. Zhai, The grain size-dependent electrical properties of  $\text{Bi}_4\text{Ti}_3\text{O}_{12}$  piezoelectric ceramics, *J. Alloys Compd.* 551 (2013) 92–97.
- [29] A. Khokhar, M.L.V. Mahesh, A.R. James, Parveen K. Goyal, K. Sreenivas, Sintering characteristics and electrical properties of  $\text{BaBi}_4\text{Ti}_4\text{O}_{15}$  ferroelectric ceramics, *J. Alloys Compd.* 581 (2013) 150–159.
- [30] J. Tellier, Ph. Boullay, M. Manier, D. Mercurio, A comparative study of the Aurivillius phase ferroelectrics  $\text{CaBi}_4\text{Ti}_4\text{O}_{15}$  and  $\text{BaBi}_4\text{Ti}_4\text{O}_{15}$ , *J. Solid State Chem.* 177 (2004) 1829–1837.
- [31] A.L. Kholkin, M. Avdeev, M.E.V. Costa, J.L. Baptista, Dielectric relaxation in Ba-based layered perovskites, *App. Phys. Lett.* 79 (2001) 662–664.
- [32] H. Irie, M. Miyayama, T. Kudo, Electrical properties of a bismuth layer structured  $\text{Ba}_2\text{Bi}_4\text{Ti}_5\text{O}_{18}$  single crystal, *J. Am. Ceram. Soc.* 83 (2000) 2699–2704.
- [33] W. Luan, L. Gao, J. Guo, Size effect on dielectric properties of fine-grained  $\text{BaTiO}_3$  ceramics, *Ceram. Int.* 25 (1999) 727–729.
- [34] L. Wu, M.C. Chure, K.K. Wu, W.C. Chang, M.J. Yang, W.K. Liu, M.J. Wu, Dielectric properties of barium titanate ceramics with different materials powder size, *Ceram. Int.* 35 (2009) 957–960.
- [35] P. Ferrer, M. Alguero, A. Castro, Influence of the mechanochemical condition on the processing of  $\text{Bi}_4\text{SrTi}_4\text{O}_{15}$  ceramics from submicronic powdered precursors, *J. Alloys Compd.* 464 (2008) 252–258.
- [36] S.M.Aygun, Processing Science of Barium Titanate, (<http://www.lib.ncsu.edu/resolver/1840.16/5489>).
- [37] H. Zhang, H. Yan, H. Ning, M.J. Reece, M. Eriksson, Z. Shen, Y. Kan, P. Wang, The grain size effect on the properties of Aurivillius phase  $\text{Bi}_{3.15}\text{Nd}_{0.85}\text{Ti}_3\text{O}_{12}$  ferroelectric ceramics, *Nanotechnology* 20 (385708) (2009) 5.